Microbial survival and heat generation during online sterilization of cheese whey in conventional and coil photo-reactors

A.E. Ghaly* and J.P. Singh

*Department of Process Engineering and Applied Science, Dalhousie University, P.O. Box 1000, Halifax, Nova Scotia B3J 2X4, Canada. *Email: abdel.ghaly@dal.ca*

Ghaly, A.E. and Singh, J.P. 2007. **Microbial survival and heat generation during online sterilization of cheese whey in conventional and coil photo-reactors**. Canadian Biosystems Engineering/Le génie des biosystèmes au Canada **49**: 3.1 - 3.12. The performance of a newly designed coil UV reactor was investigated and compared to a conventional UV reactor for the purpose of online sterilization of cheese whey. The microbial destruction efficiencies as well as the heat balances of both the reactors were investigated at eleven flow rates (5, 10, 15, 20, 25, 30, 35, 40, 50, 60, and 70 mL/min). Although the flow was laminar in both the reactors (R_e = 1.4-20.1), Dean vortices were observed in the coil reactor (D_e= 1.1-15.4) which resulted in higher destruction efficiencies and increased heat transfer. The coil reactor achieved higher microbial destruction in a shorter retention time. The rate of microbial destruction was described by exponential and polynomial equations for the conventional and coil reactors, respectively. Increasing the flow rate from 5 to 70 mL/min decreased the microbial destruction efficiency of the conventional reactor from 99.40 to 31.58% while the microbial destruction efficiency in the coil reactor increased from 60.77% at the 5 mL/min flow rate to 99.98% at the 30 mL/min flow rate and then decreased with further increases in flow rate reaching 46.2% at the 70 mL/min flow rate. The temperature of the effluent decreased with the increase in flow rate in both reactors. The maximum effluent temperatures in the conventional and coil reactors were 45.8 and 46.1 °C, respectively. The results indicated that in both reactors a major portion of the heat (23.6-77.4%) was lost with cheese whey effluent while small losses occurred through the reactor wall (1.1-44.4%) and top (0.1-1.2%). Heat generation increased with increase in flow rate in both reactors but the heat losses were more in the coil reactor compared to the conventional reactor due to the presence of the helical coil. The effective radiation decreased (from 52.82 to 7.33 kJ/h in the conventional reactor and from 49.20 to 4.51 kJ/h in the coil reactor) with the increase in flow rate (from 5 to 70 mL/min) in both reactors. The observed fouling in the coil reactor was significantly less compared to the conventional reactor. **Keywords:** cheese whey, coil, conventional, sterilization, UV, reactor, temperature, heat generation.

Les performances d'un nouveau design de réacteur UV à serpentins pour la stérilisation en continu de petit lait ont été évaluées et comparées à celles d'un réacteur UV conventionnel. L'efficacité de destruction microbienne ainsi que le bilan de chaleur des deux types de réacteurs ont été évalués à onze débits (5, 10, 15, 20, 25, 30, 35, 40, 50, 60 et 70 mL/min). Même si l'écoulement était laminaire dans les deux réacteurs (R_e = 1.4-20.1), des vortex de Dean ont été observés dans le réacteur à serpentins (D_e = 1.1-15.4) résultant en une plus grande efficacité de destruction et un transfert de chaleur accru. Le réacteur à serpentins a permis une plus importante destruction microbienne pour un temps de rétention réduit. Le taux de destruction microbienne a été représenté par des équations exponentielles et polynominales pour les réacteurs conventionnel et à serpentins, respectivement. Une augmentation du débit de 5 à 70 mL/min a diminué l'efficacité de destruction microbienne du réacteur conventionnel de 99,40 à 31,58% alors que l'efficacité de destruction microbienne dans le réacteur à serpentins augmentait de 60,77% à un débit de 5 mL/min à 99,98% à un débit de 30 mL/min et ensuite diminuait avec des augmentations plus marquées du débit pour atteindre 46,2% à un débit de 70 mL/min. Dans les deux réacteurs, la température de l'effluent diminuait avec une augmentation du débit. Les températures maximales de l'effluent dans le réacteur conventionnel et le réacteur à serpentins étaient de 45,8 et 46,1^{0}C, respectivement. Les résultats ont indiqué que, dans les deux réacteurs, la plus grande partie de la chaleur (23,6-77,4%) était perdue avec l'effluent de petit lait alors que des pertes plus faibles survenaient au niveau des parois (1,1-44,4%) et du sommet (0,1-1,2%) du réacteur. La production de chaleur augmentait avec une augmentation du débit dans les deux réacteurs mais les pertes de chaleur étaient supérieures dans le réacteur à serpentins comparativement au réacteur conventionnel dues à la présence du serpentin hélicoïdal. La radiation résultante diminuait (de 52,82 à 7,33 kJ/h dans le réacteur conventionnel et de 49,20 à 4,51 kJ/h dans le réacteur à serpentin) avec une augmentation du débit (de 5 à 70 mL/min) dans chacun des réacteurs. L'encrassement observé dans le réacteur à serpentins était significativement moindre comparativement au réacteur conventionnel. **Mots clés**: petit lait, serpentin, conventionnel, stérilisation, UV, réacteur, température, production de chaleur.

INTRODUCTION

Cheese whey is a greenish–yellow watery by-product of the cheese making process. It contains about 93% water, 5% lactose, 0.9% protein, 0.3% fat, 0.2% lactic acid, and small amounts of vitamins (Ben-Hassan et al. 1993). Because of its high biochemical oxygen demand (40-60 g/L), disposal of cheese whey has created major problems for the dairy industry. (Marshall and Harper 1984; Singh and Ghaly 1988; Ghaly and El -Taweel 1995; Mahmoud and Ghaly 2004). Using cheese whey in fermentation systems for the production of value added products for animal and human consumption requires sufficient treatment in order to kill the undesirable micro-organisms present in it.

Thermal treatment (pasteurization) of cheese whey has been found to be very time consuming and can denature the whey protein (Ghaly and El-Taweel 1995). In order to save time while

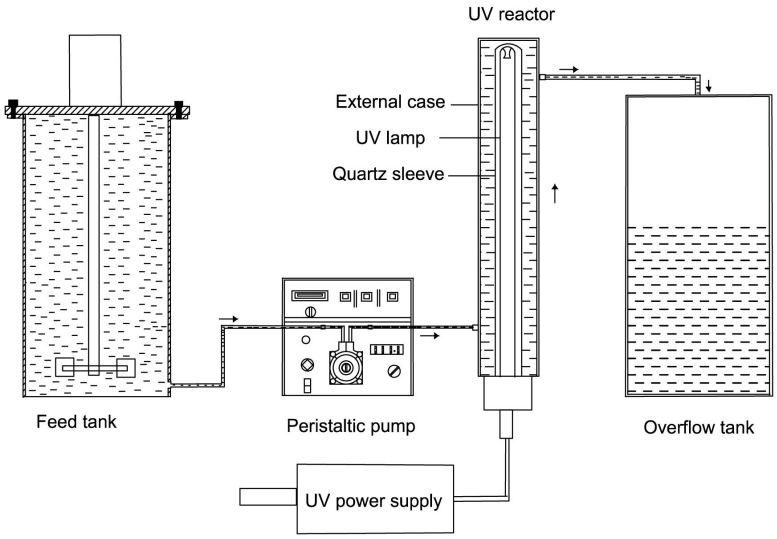

Fig. 1. Experimental setup.

ensuring complete destruction of micro-organisms, a continuous sterilization technique for cheese whey using UV-C radiation has been suggested by Mahmoud and Ghaly (2004) and Singh and Ghaly (2006). UV radiation in the spectrum of 180-320 nm has a germicidal effect with the optimum at 265 nm (Miller et al. 1999). Ultraviolet radiation has been extensively used in many applications such as drinking water disinfection (Qualls et al. 1983), medical devices sterilization (Khomich et al. 1998), air disinfection (Van Osdell and Foarde 2002), and juice pasteurization (McCandless 1998).

However, UV lamps are known to generate heat during their operation, which raises the temperature of the liquid material being sterilized. Blatchley (1997) reported that 50% of the energy input of a typical 65 W low pressure mercury lamp is converted into UV radiation while the rest is converted into heat. Mahmoud and Ghaly (2004) reported that conventional UV reactors in which the flow is laminar produces a significant amount of heat that causes fouling. In an effort to minimize fouling during cheese whey sterilization using conventional UV reactors, they decreased the gap size (flow thickness) in order to reduce the heat generated by a low pressure UV lamp.

To create mixing while maintaining a low flow rate (long retention time), Dean flow has been suggested by Singh and Ghaly (2006). The phenomenon of Dean flow refers to a secondary flow caused by flow movement in curved tubes (Brewster et al. 1993). The secondary flow is the double spiral motion produced by a gradual bend in a closed passage (bent pipe or curved pipe). The direction of the secondary flow is perpendicular to the main direction of flow. Dean vortices resulting from flow in helical tubes are known to be an effective means of heat and mass transfer enhancement (Ghogomu et al. 2001; Rane and Tandale 2005) and have been used to reduce concentration polarization and membrane fouling during nano-filtration (Mallubhotla and Belfort 1997).

OBJECTIVES

The aim of this study was to evaluate the destruction efficiency of conventional and coil UV reactors and to determine the rates of heat generation and removal during continuous sterilization of cheese whey in these reactors. The specific objectives were to determine: (a) the relationship between survival ratio and residence time, (b) the temperature variations of the flowing cheese whey inside the reactors, (c) the heat generated by the UV lamp and the various heat losses through the reactor, and (d) the impact of the temperature on fouling.

MATERIAL and METHODS

Experimental apparatus

The experimental set up (Fig. 1) consisted of UV reactors, cheese whey feeding, effluent removal system, and a data logger.

Two 380-mm arc length low pressure mercury lamps each enclosed in a 21-mm diameter (OD) quartz tube were used in two UV reactors. The radiant energy of the lamps was 160 J/m^2 at 95 UV transmittance . The inner and the outer diameters of both reactors were 55 and 61 mm, respectively. A 3-mm thick stainless steel chamber gave a gap size (distance between the quartz sleeve and the inner surface of reactor casing) of 17 mm in both reactors. A coil made of stainless steel, with a length of 448 mm, a thickness of 0.85 mm, and a pitch of 20 mm, was used to create Dean flow in one of the reactors. The outlet of the coil reactor was 13.4 mm above the outlet of the conventional reactor in order to compensate for the volume occupied by the coil and thus give the same working volume of 840 mL in both reactors. Figure 2 shows the geometry of the two UV reactors.

The feeding and effluent removal system consisted of a feeding tank, feeding pumps, and an effluent collection tank. The feeding tank (11 L) was made of a plexiglas cylinder of 4-mm wall thickness, 200-mm ID, and 435-mm height. The bottom and cover of the feeding tank were made of 4-mm thick plexiglas circular plates. A mixing shaft having stirring paddles (1.5-mm thick and 72-mm length) of 9-mm diameter and a 370.5-mm length was installed through the center of the feeding tank cover and driven by an electric motor (Model 5935932, Type NSI-10RS3, Bodine Electric Company, Chicago, IL) mounted on top of the feeding tank cover. The outlet port (4-mm diameter) of the feeding tank was located 15 mm from the bottom. Two variable speed peristaltic pumps and Masterflex precision tubing (Digi-Staltic, Masterflex model 7253-60, head model 77200-50, tubing no. EL-06429-14, Barnant Company, Barrington, IL) were used to pump the material from the feeding tank into the UV reactors. A 10-L effluent collection tank was made from 4-mm thick plexiglas cylinder of 200-mm ID and 390-mm height. The cover and the bottom of the overflow tank were made from 4-mm thick plexiglas plates of 210-mm diameter.

A Digital datalogger (Model 4702-5 E, Cole Parmer, Chicago, IL) was used to record the temperature changes in the reactors. The temperature was measured using type T thermocouples at nine different locations as shown in Fig. 2: (a) the outside surface of the reactor opposite the inlet, (b) the outside surface of the reactor at the mid-height, (c) the outside surface of the reactor opposite the outlet, (d) the reactor head space, (e) the inside surface of the reactor top, (f) the outside surface of the reactor top, (g) the outlet, (h) the inlet, and (i) the lamp socket surface.

Legend for temperatures
Ta - laboratory air temperature
1 - temperature on outside surface of reactor opposite inlet
2 - temperature on outside surface of reactor at mid-height
3 - temperature on outside surface of reactor opposite outlet
4 - temperature of reactor head space
5 - temperature on inside surface of reactor top
6 - temperature on outside surface of reactor top
7 - outlet cheese whey temperature
8 - inlet cheese whey temperature
9 - temperature of lamp socket surface

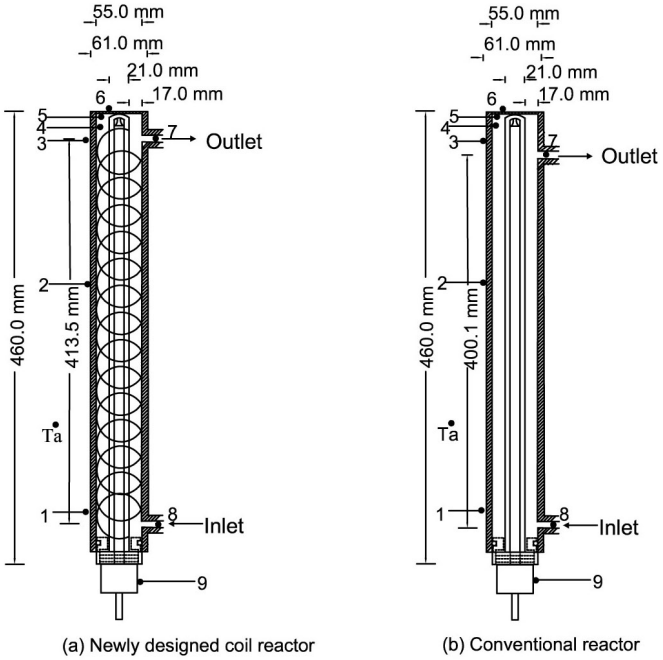

Fig. 2. Photo-reactors.

Cheese whey collection and preparation

The cheese whey used in the study was obtained from the Farmer's Cooperative Dairy Plant in Truro, Nova Scotia. A sufficient amount of cheese whey was collected in several containers and stored in the Biotechnology Laboratory at about -25°C until needed. When required for use, a few containers were withdrawn from the freezer and kept at room temperature to thaw and to increase the microbial population. Some characteristics of the cheese whey are presented in Table 1.

Experimental protocol

The performance of the two reactors were evaluated at eleven flow rates (5, 10, 15, 20, 25, 30, 35, 40, 50, 60, and 70 mL/min) which gave retention times of 168, 84, 56, 42, 33.6, 28, 24, 21, 16.8, 14, and 12 min, respectively. Before starting each experimental run, the UV reactors and all accessories (feeding tank, overflow tank, tubings) were all cleaned with detergent and hot water, and then chemically sterilized using 2% sodium metabisulfite solution to eliminate any microbial contamination. The cheese whey was pumped through the UV reactors at the required flow rates using the peristaltic pumps. The temperature readings were recorded at the different flow rates. Samples were collected from the inlet and the outlet for the plate count analysis.

Table 1. Some characteristics of the cheese whey (from Singh and Ghaly 2006).

Characteristics	Measured value	Units
Total solids (TS)	56800	mg/L
Volatile solids (VS)	47900	mg/L
VS as percent of TS	84.33	%
Ash	8900	mg/L
Ash as percent of TS	15.67	%
Total chemical oxygen demand (TCOD)	75800	mg/L
Soluble chemical oxygen demand (SCOD)	58000	mg/L
SCOD as percent of TCOD	76.52	%
Total Kjeldahl nitrogen (TKN)	1500	mg/L
Ammonium nitrogen (AN)	270	mg/L
AN as percent of TKN	18	%

Analysis

Microbial counts were performed on untreated and UV treated cheese whey samples. A plate count agar (DIFCO, 0751-17-2), which contained 5 g of bacto yeast agar dissolved in 1 L and sterilized at 121°C and 101.4 kPa for 15 min in an autoclave (model STM-E, Market Forge Sterilmatic, New York, NY) was poured into several petri dishes. Serial dilutions of 10^{-1}-10^{-7} were prepared from the samples. An aliquot of 0.1 mL of each of the dilutions was placed on the plate count agar in the petri dish (in triplicate) and gently swirled until consistently spread on the agar surface with the glass spreader. The petri dishes were incubated at 32°C in an incubator (Fisher Isotemp, Cat. No. 11-680-626, Fisher Scientific, Whitby, ON) until visible growth was observed. The visible growth of colonies was counted as colony forming units per millimeter (CFU/mL) according to the procedure described in the Standard Methods for the Examination of Dairy Products (APHA 1967).

HEAT BALANCE

A heat balance was performed on both reactors during the continuous sterilization of the cheese whey. The heat balance included: (a) the heat generated by the UV lamp, (b) the heat lost with the cheese whey effluent, (c) the heat lost through the reactor top, (d) the heat lost through the reactor bottom, (e) the heat lost through the reactor walls, and (f) the heat gained by the reactor components (Fig. 3):

$$q_u = q_e + q_t + q_b + q_w + q_r \quad (1)$$

where:

q_u = rate of heat generated by UV lamp (kJ/h),
q_e = rate of heat lost with cheese whey effluent (kJ/h),
q_t = rate of heat lost through reactor top (kJ/h),
q_b = rate of heat lost through reactor bottom (kJ/h),
q_w = rate of heat lost through reactor walls (kJ/h), and
q_r = rate of heat gained by the reactor components (kJ/h).

With reference to Fig. 4, the values of q_e, q_t, q_b, q_w, and q_r are calculated using Eqs. 2-6.

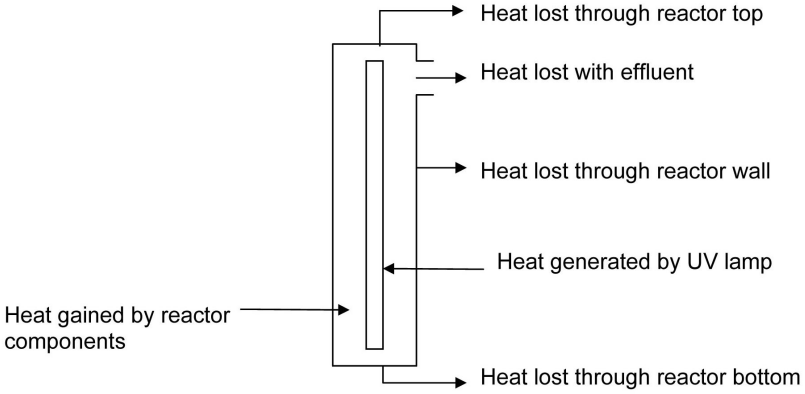

Fig. 3. Sources of heat losses/gain for the entire sterilization system.

$$q_e = MC_{pe}\left(T_{ie} - T_{oe}\right) \quad (2)$$

$$q_t = U_t A_t \left(T_{ia} - T_a\right) \quad (3)$$

$$q_b = U_b A_b \left(T_i - T_a\right) \quad (4)$$

$$q_w = U_w A_w \left(T_m - T_a\right) \quad (5)$$

$$q_r = q_{gb} + q_{gt} + q_{gw} \quad (6)$$

where:

A_b = surface area of the reactor bottom (m^2),
A_t = surface area of the reactor top (m^2),
A_w = surface area of reactor outer walls (m^2),
C_{pe} = specific heat of effluent (kJ kg^{-1} K^{-1}),
M = flow rate of effluent (kg/h),

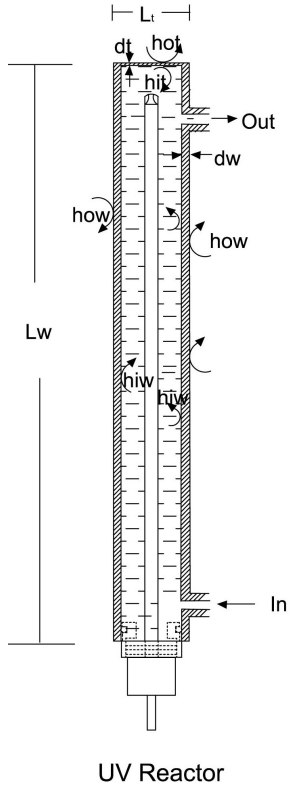

UV Reactor

Fig. 4. Heat transfer coefficients.

q_{gb} = rate of heat gained by reactor bottom (kJ/h),
q_{gt} = rate of heat gained by reactor top (kJ/h),
q_{gw} = rate of heat gained by reactor walls (kJ/h),
T_a = ambient air temperature (K),
T_i = inlet temperature of cheese whey (K),
T_{ia} = temperature of air entrapped in head space of reactor (K),
T_{ie} = inlet temperature of effluent (K),
T_m = mean temperature of cheese whey (K),
T_{oe} = outlet temperature of effluent (K),
U_b = overall heat transfer coefficient of reactor bottom (kJ m^{-2} h^{-1} K^{-1}),
U_t = overall heat transfer coefficient of reactor top (kJ m^{-2} h^{-1} K^{-1}), and
U_w = overall heat transfer coefficient of reactor walls (kJ m^{-2} h^{-1} K^{-1}).

The rate of heat gained by reactor top, bottom and walls is calculated from Eqs. 7 -9.

$$q_{gt} = \frac{m_t c_{pt}\left(T_2 - T_1\right)}{\Delta t} \quad (7)$$

$$q_{gb} = \frac{m_b c_{bt}\left(T_2 - T_1\right)}{\Delta t} \quad (8)$$

$$q_{gw} = \frac{m_w c_w \left(T_2 - T_1\right)}{\Delta t} \quad (9)$$

where:

C_{bt} = specific heat of bottom material of reactor (kJ kg^{-1} K^{-1}),
C_{pt} = specific heat of top material of reactor (kJ kg^{-1} K^{-1}),
C_w = specific heat of wall material of reactor (kJ kg^{-1} K^{-1}),
T_1 = initial temperature (K),
T_2 = final temperature (K),
Δt = time interval (h),
m_b = mass of bottom of reactor (kg),
m_t = mass of top of reactor (kg), and
m_w = mass of walls of reactor (kg).

The terms m_t, m_b, and m_w are calculated from Eqs. 10 - 12.

$$m_t = A_t d_t \rho_t \quad (10)$$

$$m_b = A_b d_b \rho_b \quad (11)$$

$$m_w = A_{dw} L_w \rho_w \quad (12)$$

where:

A_{dw} = cross-sectional area of cylinder (m^2) ,
d_b = thickness of reactor bottom (m),
d_t = thickness of reactor top (m),
L_w = characteristic length, height of reactor (m),
ρ_b = density of material of reactor bottom (kg/m^3),
ρ_t = density of material of reactor top (kg/m^3), and
ρ_w = density of the material of reactor walls (kg/m^3).

The cross-sectional area of the cylinder is calculated as:

$$A_{dw} = \pi\left(r_o^2 - r_i^2\right) \quad (13)$$

where:

r_o = outer radius of reactor (m), and

r_i = inner radius of reactor (m).

The overall heat transfer coefficient of the reactor top (U_t) is calculated as (Holman 2002):

$$U = \frac{1}{\frac{1}{h_{it}} + \frac{1}{h_{ot}} + \frac{d_t}{k_t}} \quad (14)$$

where:

h_{it} = convective heat transfer coefficient between inner surface of reactor top and air in reactor (kJ m^{-2} h^{-1} K^{-1}),

h_{ot} = convective heat transfer coefficient between outer surface of reactor top and ambient air (kJ m^{-2} h^{-1} K^{-1}), and

k_t = thermal conductivity of top material (kJ m^{-1} h^{-1} K^{-1}).

For laminar flow ($10^4 < Gr_f Pr_f < 10^9$), the convective heat transfer coefficients (h_{ot}) and (h_{it}) are calculated as (Holman 2002):

$$h_{at} = 1.32\left(\frac{T_{ot} - T_a}{L_t}\right)^{0.25} \quad (15)$$

$$h_{it} = 1.32\left(\frac{T_{ia} - T_{it}}{L_t}\right)^{0.25} \quad (16)$$

where:

$Gr_f Pr_f$ = Rayleigh number,

T_{it} = temperature of inside surface of reactor top (K),

T_{ot} = temperature of outside surface of reactor top (K), and

L_t = characteristic length, diameter of the top (m).

The value of the Prandtl number (Pr_f) is obtained from the Standard Tables (Holman 2002) while that of the Grashof number (Gr_f) is calculated using Eqs. 17 and 18.

For the outer surface:

$$Gr_f = \frac{g\beta\left(T_{ot} - T_a\right)L_t^3}{\upsilon^2} \quad (17)$$

For the inner surface:

$$Gr_f = \frac{g\beta\left(T_{ia} - T_{it}\right)L_q^3}{\upsilon^2} \quad (18)$$

where:

g = gravitational acceleration (m/s^2),

Gr_f = Grashof number,

υ = kinematic viscosity (m^2/s), and

β = volume coefficient of expansion (K^{-1}).

The film temperatures for the reactor top and inner surfaces are calculated using Eqs. 19 and 20.

$$T_f = \frac{T_{ot} + T_a}{2} \quad (19)$$

$$T_f = \frac{T_{ia} + T_{it}}{2} \quad (20)$$

where: T_f = film temperature.

For ideal gases, the volume coefficient of expansion (β) is the reciprocal of the absolute temperature of the gas while for the other fluids it is obtained from the Standard Tables (Holman 2002). For Eqs.17 and 18, the value of β is calculated from Eq. 21.

$$\beta = \frac{1}{T_f} \quad (21)$$

The overall heat transfer coefficient of the reactor bottom (U_b) is calculated as (Holman 2002):

$$U_b = \frac{1}{\frac{1}{h_{ib}} + \frac{1}{h_{ob}} + \frac{d_b}{k_b}} \quad (22)$$

where:

h_{ib} = convective heat transfer coefficient between inner surface of reactor bottom and cheese whey effluent (kJ m^{-2} h^{-1} K^{-1}),

h_{ob} = convective heat transfer coefficient between outer surface of reactor bottom and ambient air (kJ m^{-2} h^{-1} K^{-1}), and

k_b = thermal conductivity of bottom material (kJ m^{-1} h^{-1} K^{-1}).

The heat transfer from the cheese whey to the inner surface of the reactor bottom is by forced convection while that from the outside to the air is by natural convection. Since the heat transfer coefficient due to forced convection (h_{ib}) is very large compared to that of the natural convection (h_{ob}), the term ($1/h_{ib}$) will be very small and can be neglected. Thus the overall heat transfer coefficient of the reactor bottom (U_b) is rewritten as:

$$U_b = \frac{1}{\frac{1}{h_{ob}} + \frac{d_b}{k_b}} \quad (23)$$

For laminar flow ($10^4 < GrPr_f < 10^9$), the convective heat transfer coefficients (h_{ob}) is calculated as (Holman 2002):

$$h_{ob} = 0.59\left(\frac{T_{ob} - T_a}{L_b}\right)^{0.25} \quad (24)$$

where:

L_b = characteristic length of reactor bottom, diameter of bottom (m) and

T_{ob} = temperature of the surface of the bottom (K).

The value of the Prandtl number (Pr_f) is obtained from the Standard Tables (Holman 2002) while that of the Grashof number (Gr_f) is calculated using:

$$Gr_f = \frac{g\beta\left(T_{ob} - T_a\right)L_b^3}{\upsilon^2} \quad (25)$$

where β is calculated from Eq. 21.

The film temperature is calculated as:

$$T_f = \left(\frac{T_{ob} + T_a}{2}\right) \quad (26)$$

Table 2. Values of the various parameters used in the heat balance calculations for the conventional and coil reactors.

Parameter	Value	Units
A_{iw}	79482.29	mm^2
A_{ow}	88153.08	mm^2
A_t	2922.0	mm^2
C_{pe}	4.17	kJ kg^{-1} °C^{-1}
d_t	2.00	mm
d_w	3.00	mm
g	9.81	m/s^2
k_t	47.6	W m^{-1} °C^{-1}
k_w	47.6	W m^{-1} °C^{-1}
L_t	61.0	mm
L_w	460.00	mm
r_o	30.50	mm
r_i	27.50	mm

The overall heat transfer coefficient of the reactor wall (U_w), based on the outside area of the cylinder, is calculated as (Holman 2002):

$$U_w = \frac{1}{\frac{1}{h_{ow}} + \frac{1}{h_{iw}}\left(\frac{A_{ow}}{A_{iw}}\right) + \frac{A_{ow}\ln\left(r_0 / r_i\right)}{2\pi k_w L_w}} \quad (27)$$

where:

A_{iw} = surface area of inside wall of reactor (m^2),
A_{ow} = surface area of outside wall of reactor (m^2),
h_{iw} = convective heat transfer coefficient between cheese whey and reactor inside wall (kJ m^{-2} h^{-1} K^{-1}),
h_{ow} = convective heat transfer coefficient between reactor outside wall and ambient air (kJ m^{-2} h^{-1} K^{-1}), and
k_w = thermal conductivity of cylindrical wall (kJ m^{-1} h^{-1} K^{-1}).

The heat transfer from the cheese whey to the inner surface of the reactor wall is by forced convection, while that from the outer surface to the air is by natural convection. Since the heat transfer due to forced convection (h_{iw}) is very large compared to that of the natural convection (h_{ow}), the term ($1/h_{iw}$) (A_{ow}/A_{iw}) will be very small and can be neglected. Thus Eq. 27 is rewritten as:

$$U_w = \frac{1}{\frac{1}{h_{ow}} + \frac{A_{ow}\ln\left(r_o / r_i\right)}{2\pi k_w L_w}} \quad (28)$$

For laminar flow ($10^4 < Gr_f Pr_f < 10^9$), the convective heat transfer coefficients (h_{ow}) is calculated as (Holman 2002):

$$h_{ow} = 1.42\left(\frac{T_{ow} - T_a}{L_w}\right)^{0.25} \quad (29)$$

where: T_{ow} = temperature of outer surface of reactor wall (K).

The value of the Prandtl number (Pr_f) is obtained from the Standard Tables (Holman 2002) while that of tthe Grashof number (Gr_f) is calculated using:

$$Gr_f = \frac{g\beta\left(T_{ow} - T_a\right)L_w^3}{\upsilon^2} \quad (30)$$

For Eq. 30, the value of β is obtained from tables Holman 2002). The film temperature in this case is calculated as:

$$T_f = \frac{T_{ow} + T}{2} \quad (31)$$

The values of the various parameters used in the heat balance calculations are presented in Table 2.

RESULTS and DISCUSSION

Microbial survival

The final microbial populations in the effluents and the destruction efficiencies of the conventional and coil reactors are shown in Table 3. The results are the average of the three replicates. The coefficient of variation varied from 0.0 to 9.3%. The survival curves for both reactors are shown in Fig. 5.

Table 3. Effect of flow rate on final cell number, destruction efficiency, and Dean number.

Flow rate (mL/min)	Residence time (min)	Reynolds number* (*Re*)	Dean number** (*De*)	Conventional reactor		Coil reactor	
				Final cell number (x 10^6)	Destruction efficiency (%)	Final cell number (x 10^6)	Destruction efficiency (%)
5	168.0	1.39	1.09	0.046	99.40	2.903	60.77
10	84.0	2.79	2.23	0.122	98.40	2.314	69.52
15	56.0	4.18	3.34	0.236	96.90	1.096	85.56
20	42.0	5.58	4.46	0.547	92.80	0.285	96.24
25	33.6	6.97	5.57	1.003	86.80	0.125	98.35
30	28.0	8.37	6.69	1.718	77.40	0.002	99.98
35	24.0	9.70	7.76	2.364	68.90	0.008	90.90
40	21.0	11.16	8.93	3.010	60.40	0.437	75.80
50	16.8	13.95	11.16	4.028	47.00	1.830	53.51
60	14.0	16.75	13.40	4.669	38.56	3.800	50.51
70	12.0	20.10	15.41	5.200	31.58	4.080	46.20

Initial cell number is 7.6 x 10^6 cells/mL
* For both reactors
** For coil reactor

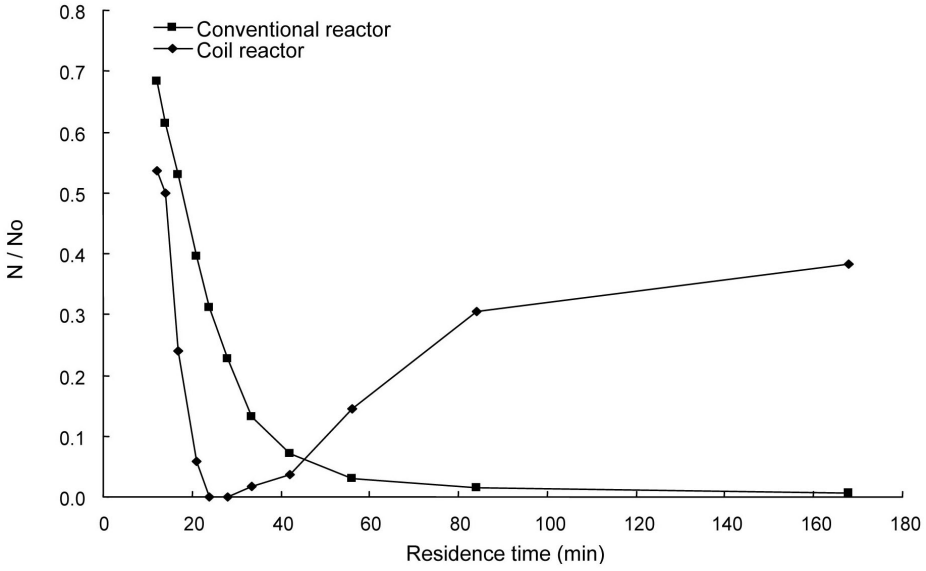

Fig. 5. Survival curves for the coil and conventional reactors.

Survival curves are plots of the ratio of the concentration of the final number of microorganisms found after the treatment (N) to the initial number of microorganisms (N_o) and are used to interpret the inactivation kinetics of microorganisms. For the conventional reactor, the survival curve is described by:

$$\frac{N}{N_o} = \exp(-0.0319t) \tag{32}$$

while for the coil reactor the relationship is:

$$\frac{N}{N_o} = 2.137 - 0.196t + 6.5\times10^{-3}t^2 - 1\times10^{-4}t^3 + 8\times10^{-7}t^4 - 3\times10^{-9}t^5 + 6\times10^{-12}t^6 \tag{33}$$

Based on Eqs. 32 and 33, it would require more than 496 minutes (1.69 mL/min) to destroy the whole initial population in cheese whey in the conventional reactor while the optimum residence time is 28 minutes (30 mL/min) in the coil reactor. Mahmoud and Ghaly (2004) found that the destruction of microbial cells present in cheese whey in conventional UV reactors could be described by a first order equation. Koch (1995) and Mitscherlich and Marth (1984) reported that microorganisms exposed to ultraviolet germicidal irradiation (UVGI) experience an exponential decrease in population similar to other methods of disinfection such as heating, ozonation, and exposure to ionizing radiation.

Generally the flow is laminar when the Reynolds number (Re) is less than 4000 and is turbulent when it is greater than 4000 (Cengel 2003). Reynolds number calculations were performed on conventional and coil reactors using Eqs. 34 - 37.

$$Re = \frac{Ud_h}{\upsilon} \tag{34}$$

$$d_h = d_o - d_i \tag{35}$$

$$U = \frac{q}{A_c} \tag{36}$$

$$A_c = \frac{\pi\left(d_o^2 - d_i^2\right)}{4} \tag{37}$$

where:

A_c = annular section area (m^2),
d_h = hydraulic diameter (m),
d_i = inner diameter (m),
d_o = outer diameter (m),
q = volumetric flow rate (m^3/s),
Re = Reynolds number, and
U = mean velocity (m/s).

The results (Table 3) show that the Reynolds number was 1.39 for the lowest flow rate of 5 mL/min and 20.1 for the highest flow rate of 70 mL/min, indicating that the flow was laminar in both reactors.

Dean number has been used as a measure of the magnitude of the secondary flow and is calculated from Eqs. 38-41 (Nemeth and Bucsky 1997).

$$De = Re\left(\frac{r^x}{\Gamma}\right)^{0,5} \tag{38}$$

$$r^x = \frac{a}{2}\left(\frac{1}{2} - \frac{2\delta}{\pi a}\right)^{0.5} \tag{39}$$

$$\Gamma = \frac{r^2 + b^2}{r} \tag{40}$$

$$b = \frac{h}{2\pi} \tag{41}$$

where:

a = tube diameter (m),
b = a parameter (m),
h = pitch of screw line (m),
r = tube radius (m),
r^x = radius of circle having same surface as area of half cross-section beside static element (m),
Γ = radius of curvature of spherical line cut out by helical element from tubular housing (m), and
δ = thickness of coil (m).

The critical Dean number for the coil reactor was found to be 1.09 at 5 mL/min and 15.41 at 70 mL/min. The L/d was found to be 1.01. These results indicate the existence of secondary flows due to the helical nature of the flow. Webster and Humphrey (1997) stated that the two counter-rotating vortices (Dean vortices) will be present in helical pipes, even for the most mildly curved pipe. The secondary flow started to develop in the coil reactor at a Reynolds number of less than 20. The results also indicate that as the flow rate increases, the magnitude of the secondary flow increases resulting in an increase of the critical Dean number.

Low flow rates in the coil reactor did not produce a secondary flow and as a result the coil shielded the microorganisms from the UV radiation. However, the microbial

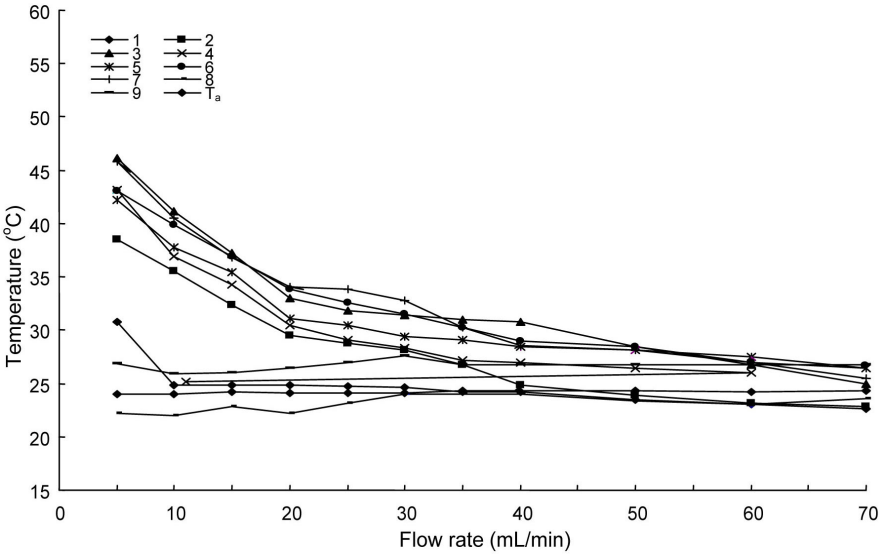

(a) Conventional reactor

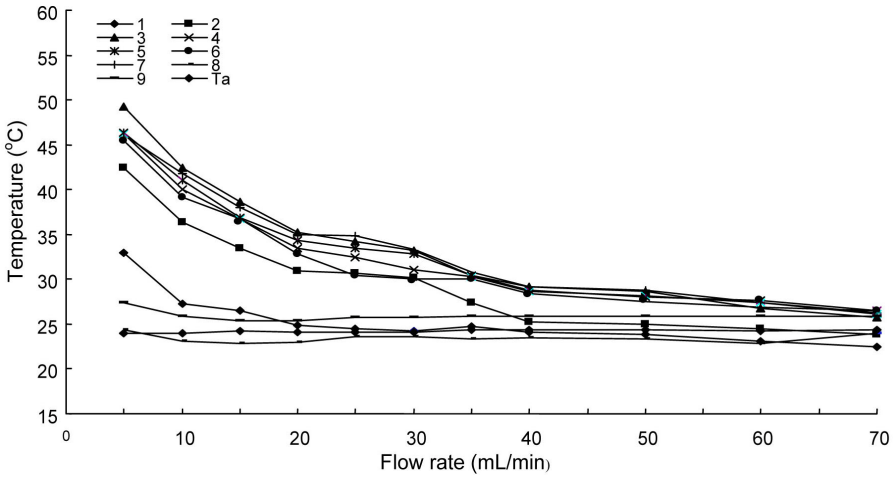

(b) Coil reactor

Fig. 6. Effect of flow rate on the steady-state temperatures (locations of thermocouples are shown in Fig. 2.)

destruction efficiency of the coil reactor increased as a result of the development of the secondary flow which caused mixing that increased the exposure of microorganisms to UV radiation. On the other hand, a flow rate greater than 39 mL/min resulted in a residence time that was too short for microbial destruction.

Temperature

Figure 6 shows the variation of steady-state temperature with flow rate in the conventional and coil reactors. The temperatures at all locations in the conventional and coil reactors decreased with increase in flow rate, except for the influent temperature (location 8), which remained constant. At steady state, the temperatures measured near the bottom of the reactors were less than the temperatures measured at the top. This was because the liquid (which was kept at room temperature) entered the reactor at the bottom and picked up heat from the lamp as it traveled upward to the outlet. It was also noticed that the temperatures measured at all the locations in the coil reactor were slightly higher than those measured at similar locations in the conventional reactor. This could be due to the mixing created by Dean vortices.

The steady state effluent temperature (location 7) decreased from 45.8°C at 5 mL/min to 25.5°C at 70 mL/min in the conventional reactor and from 46.1°C at 5 mL/min to 26.2°C at 70 mL/min in the coil reactor. The outlet temperature reported in the literature for various UV reactors varied from 10 to 62.8°C (Koutchma et al. 2004; Tran and Farid 2004; Mahmoud and Ghaly 2004; Abu-Ghararah 1994). According to the environmental technology verification program conducted by the EPA (USEPA 2002) on UV reactors produced by Trojan Technologies Incorporated (London,ON), the temperature of the effluent will vary depending on the flow rate and the reactor geometry.

Heat balance

The heat losses from the bottom of the reactors were neglected because: (a) the area of reactor bottom was very small and (b) the cheese whey inlet temperature was similar to the ambient air temperature. The heat gained by the reactor components (q_r) was also ignored as there was no other external source of heat other than the lamp. Therefore, Eq. 1 was rewritten as:

$$q_u = q_e + q_r + q_w \tag{42}$$

Since the temperature of the reactor head space (T_{ia}) and the temperature of the inside surface of the reactor top (T_{it}) were almost the same, the convective heat transfer coefficient between the inner surface of the top and the air entrapped inside the reactor (h_{it}) was ignored. The calculated Rayleigh number for the wall outer and inner surfaces (Eqs. 17 and 18) and the top (Eq. 29) for the reactors at the flow rates of 5-70 mL/min was less than 1 x 10^9 indicating that the flow was laminar. Equations 15, 28, 14, and 26 were used to calculate h_{ot}, h_{ow}, U_t, and U_w, respectively. While Eqs. 2, 5, and 3 were used to calculate q_e, q_w, and q_3, respectively.

Table 4 shows the calculated values of the various heat transfer coefficients during steady state in the reactors. The results show that the heat transfer coefficients of the coil reactor were higher than those of the conventional reactor. Rane and Tandale (2005) stated that the use of bends results in enhancement in heat transfer due to secondary flows induced in the bends. Nemeth and Bucsky (1997) indicated that the secondary flow present in curved-tube flow causes a marked variation in local transfer coefficients around the periphery of the tube.

Table 5 presents the calculated values of the various steady state heat losses and the distribution of the total energy input in

Table 4. Values of the heat transfer coefficients at the steady state conditions for the conventional and coil reactors.

Coefficient ($kL\ m^{-2}\ °C^{-1}\ h^{-1}$)	Reactor type	Flow rate (mL/min)										
		5	10	15	20	25	30	35	40	50	60	70
h_{ot}	Conventional	0.33	0.32	0.30	0.28	0.26	0.25	0.25	0.25	0.24	0.22	0.21
	Coil	0.34	0.32	0.31	0.31	0.27	0.29	0.27	0.26	0.25	0.25	0.23
h_{ow}	Conventional	0.19	0.18	0.17	0.15	0.14	0.14	0.13	0.13	0.13	0.13	0.05
	Coil	0.21	0.19	0.18	0.16	0.15	0.15	0.14	0.13	0.13	0.12	0.07
$\underline{U_t}$	Conventional	0.33	0.31	0.30	0.28	0.26	0.25	0.25	0.25	0.24	0.22	0.21
	Coil	0.34	0.32	0.31	0.30	0.28	0.27	0.26	0.26	0.25	0.24	0.23
U_w	Conventional	0.19	0.18	0.17	0.16	0.14	0.13	0.13	0.13	0.13	0.12	0.05
	Coil	0.21	0.19	0.18	0.17	0.15	0.15	0.14	0.14	0.13	0.13	0.07

Table 5. Distribution of energy input during the steady state stage for the conventional and coil reactors.

Energy (kJ/h)	Reactor type	Flow rate (mL/min)										
		5	10	15	20	25	30	35	40	50	60	70
q_e	Conventional	25.45	40.26	52.36	55.92	63.52	68.62	70.40	72.80	75.11	77.38	81.45
	Coil	27.22	46.71	56.95	59.94	69.94	72.68	74.16	75.89	78.86	80.50	83.60
q_w	Conventional	10.63	8.46	7.66	6.19	3.78	3.26	2.89	2.38	2.30	1.48	1.20
	Coil	12.26	8.55	7.90	6.54	4.50	3.81	3.10	2.56	2.30	2.00	1.80
q_t	Conventional	1.10	0.71	0.57	0.34	0.21	0.16	0.07	0.07	0.05	0.03	0.02
	Coil	1.32	0.87	0.69	0.47	0.33	0.27	0.24	0.20	0.18	0.11	0.09
q_l*	Conventional	37.18	49.43	60.59	62.45	67.51	72.04	73.36	75.25	77.46	78.89	82.67
	Coil	40.80	56.13	65.14	66.95	74.77	76.76	77.50	78.65	81.34	82.61	85.49
UV**	Conventional	52.82	40.57	29.41	27.55	22.49	17.96	16.64	14.75	12.54	11.11	7.33
	Coil	49.20	33.87	24.46	23.05	15.23	13.24	12.50	11.35	8.66	7.39	4.51

* Energy converted to heat $q_l = q_e + q_w + q_t$

** UV radiation = total energy input (108 kJ/h) - total energy converted to heat (q_l) - total energy lost in ballast (18 kJ/h as stated by manufacturer)

the conventional and coil UV reactors. A major portion of heat was lost with the cheese whey effluent (23.6-75.4% in conventional reactor and 25.2-77.4% in coil reactor) while some losses were through the reactor wall (1.1-9.8% in conventional reactor and 1.7-11.4% in coil reactor) and very small losses were from the reactor top (0.2-1.0% in conventional reactor and 0.1-1.2% in coil reactor) depending on the flow rate. The rate of heat lost with the effluent increased with increased flow rate whereas the rate of heat losses through the reactor walls and top decreased with increases in flow rate for the conventional and coil reactors. As the flow rate increased, both the average temperature of the cheese whey effluent and the temperature of the air entrapped in the head space of the reactor decreased (and consequently the differences between the average cheese whey temperature and ambient air and between the air inside the head space and the ambient air decreased) leading to less heat transfer. Blatchley and Peel (2001) and Mahmoud and Ghaly (2004) stated that the greater the volume passed through the UV reactor, the greater the heat removed.

The results also indicate that the heat losses through the effluent, walls, and top of the coil reactor were more than those of the conventional reactor. Nemeth and Bucsky (1997) stated that helical and spiral coils are often used for transferring heat in mixing, storage, and reactor vessels, as well as in process heat exchangers. The calculated values of the output heat per unit volume of the flowing cheese whey in both reactors are shown in Fig. 7. The heat gain per unit volume in both the reactors decreased with increased flow rate. Greater flow rates in the coil and conventional reactors resulted in lesser contact time of the fluid with the UV lamp thus causing less heat gain per unit volume.

According to the manufacturer (Trojan Technologies, London, ON), approximately 18 kJ/h of the energy input is lost in the ballast. Part of the remaining 90 kJ/h is converted to UV radiation at a wavelength of 257.3 nm while the rest is radiated at other wavelengths and ultimately ends up as heat. Some of the radiated UV radiation is consumed in photochemical reactions and the rest is also converted to heat. The fraction of energy converted to heat increases with increases in flow rate in both reactors (Table 5). As a result, the effective radiation which is

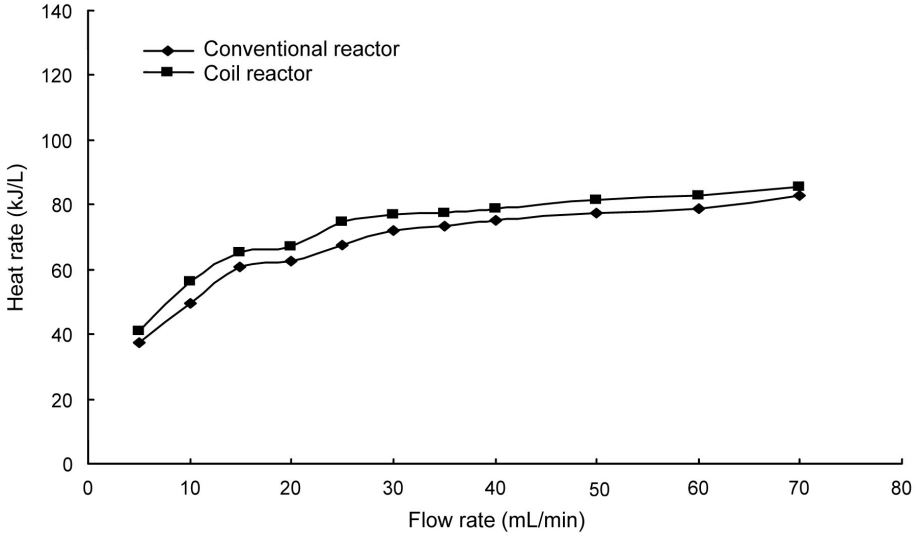

(a) Heat output rate

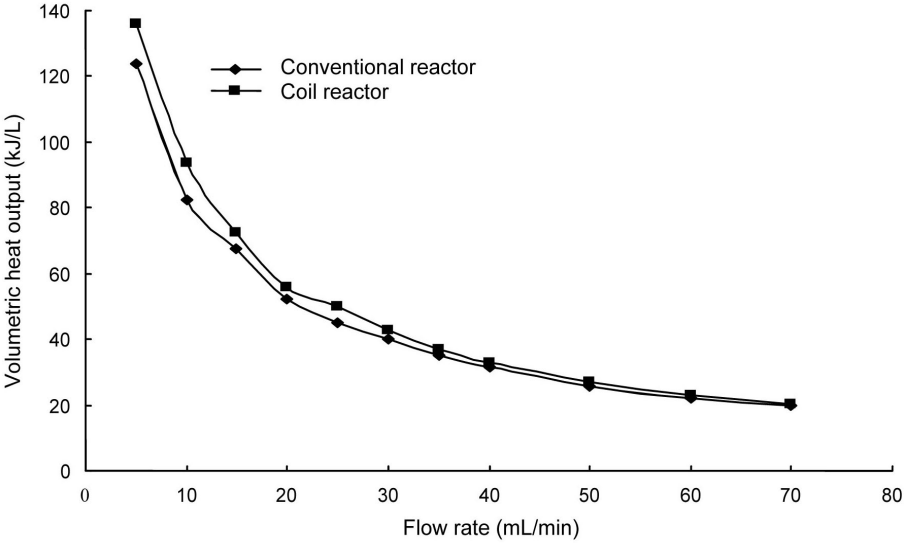

(b) Volumetric heat output

Fig. 7. Output heat per unit volume of flowing cheese whey in conventional and coil reactors.

(a) Conventional reactor

(b) Coil reactor

Fig. 8. Photographs showing fouling on UV lamps of photo-reactors.

consumed in a photochemical reaction decreased with increase in flow rate. In their study on heat generation and its impact on lamp fouling during cheese whey sterilization using a conventional UV reactor, Mahmoud and Ghaly (2004) found that the heat generated by a low pressure mercury arc lamp decreased while the effective radiation that is consumed in the photochemical reaction increased with decreasing flow.

Fouling

Suspended particles and high turbidity of the liquid medium have been found to reduce the penetration ability of the UV light and thus reduce the efficiency of the UV conventional reactor (Mahmoud and Ghaly 2004). Similarly, microorganisms can aggregate or clump together, forming particles that potentially protect microorganisms within aggregates that would otherwise be inactivated (USEPA 1999). Visual observation of the UV lamps revealed less fouling in the coil reactor compared to conventional reactor (Fig. 8). As a result of secondary flow in the coil reactor, the hydraulics of the flow differed from that in the conventional reactor and resulted in less fouling.

CONCLUSION

The coil reactor was found to be more efficient than the conventional reactor as it resulted in higher microbial destruction in shorter retention time. The destruction efficiency of the conventional reactor decreased from 99.4% (at 5 mL/min) to 31.58% (at 70 mL/min), whereas the destruction efficiency in the coil reactor increased from 60.77% (at 5 mL/min) to 99.98% (at 30 mL/min) and then decreased with further increases in flow rate reaching 46.2% (at 70 mL/min). The rate of microbial destruction was found to be exponential in the conventional reactor and polynomial in the coil reactor. The flow was laminar in both reactors (Re = 1.4 - 20.1). Dean flow was observed in the coil reactor (De = 1.09 - 15.41) and Dean vortices resulted in higher destruction efficiencies and increased heat transfer as compared to the conventional reactor. The maximum effluent temperatures in the conventional reactor and coil reactor were 45.8 and 46.1 °C, respectively. The heat generation and thus effective radiation that was consumed in the photochemical reaction in the conventional and coil reactors was

affected by flow rate. The portion of input energy that was converted to heat increased from 37.18 to 82.67 kJ/h in the conventional reactor and from 40.80 to 85.49 kJ/h in the coil reactor when flow rate was increased from 5 to 70 mL/min. The heat gain per unit volume of the flowing cheese whey decreased from 123.93 to 19.68 kJ/L in the conventional reactor and from 136.0 to 20.35 kJ/Lin the coil reactor when the flow rate was increased from 5 to 70 mL/min. The effective UV radiation decreased from 52.82 to 7.33 kJ/h in the conventional reactor and from 49.20 to 4.51 kJ/h in the coil reactor when the flow rate was increased from 5 to 70 mL/min. Fouling in the coil reactor was less compared to the conventional reactor.

ACKNOWLEDGEMENT

This research was funded by the Natural Sciences and Engineering Research Council of Canada (NSERC).

REFERENCES

Abu-Ghararah, Z.H. 1994. Effect of temperature on the kinetics of wastewater disinfection using ultraviolet radiation. *Journal of Environmental Science and Health* A29 (3): 585-603.

APHA. 1967. *Standard Methods for the Examination of Dairy Products*. Washington, DC: American Public Health Association.

Ben-Hassan, R.M., A.E. Ghaly and N. Ben-Abdallah. 1993. Heat generation during batch and continuous production of single cell protein from cheese whey. *Biomass and Bioenergy* 4(3): 213-225.

Blatchley, E.R.K. 1997. Numerical modeling of UV intensity: Application to collimated-beam reactors and continuous-flow systems. *Water Research* 31(9): 2205-2218.

Blatchley, E.R. and M.M. Peel. 2001. Disinfection by ultraviolet irradiation. In *Disinfection, Sterilization and Preservation*, 5th edition, ed. S.S. Block, 823 - 852. Philadelphia, PA: Lippincott Williams & Wilkins.

Brewster, M.E., K.Y. Chung and G. Belfort. 1993. Dean vortices with wall flux in a curved channel membrane system: A new approach to membrane module design. *Journal of Membrane Science* 81:127–137.

Cengel, Y.A. 2003. *Heat Transfer: A Practical Approach*, 2nd edition. Boston, MA: McGraw-Hill.

Ghaly, A.E. and A.A. El-Taweel. 1995. Effect of lactose concentration on batch production of ethanol from cheese whey using *Candida Pseudotropicalis*. *Transactions of the ASAE* 38(4): 1113-1120.

Ghogomu, J.N., C. Guigui, J.C. Rouch, M.J. Clifton and P. Aptel. 2001. Hollow-fibre membrane module design: Comparison of different curved geometries with Dean vortices. *Journal of Membrane Science* 181 (1): 71-80.

Holman, J.P. 2002. *Heat Transfer*, 9th edition. New York, NY: McGraw-Hill.

Khomich, V.A., I.A. Soloshenko, V.V. Tsiolko and I.L Mikhno. 1998. Investigation of principle factors of the sterilization by plasma DC glow discharge. In *Proceedings of ICPP & 25th EPS Conference on Controlled Fusion and Plasma Physics*, ed. P. Pavlo, Vol. 22C: 2745-2748. European Physical Society.

Koch, A.L. 1995. *Bacterial Growth and Form*. New York, NY: Chapman & Hall.

Koutchma, T., S.K. Stuart, C. Stuary and B. Parisi. 2004. Ultraviolet disinfection of juice products in laminar and turbulent flow reactors. *Innovative Food Science and Emerging Technologies* 5: 179-189.

Mahmoud, N.S. and A.E. Ghaly. 2004. On-line sterilization of cheese whey using ultraviolet radiations. *Biotechnology Progress* 20: 550-560.

Mallubhotla, H. and G. Belfort. 1997. Flux enhancement during Dean vortex microfiltration: 8. Further diagnostics. *Journal of Membrane Science* 125: 75-91.

Marshall, K.R. and W.J. Harper. 1984. Treatment of wastes from the dairy industry. In *Surveys in Industrial Wastewater Treatment*, eds. D. Barnes, C.F. Forster and S.E. Hrudey, Vol. 1: 296-376. Boston, MA: Pitman Advanced Publishing Program.

McCandless, L. 1998. Cider pasteurization via ultraviolet light (UV). http://www.nysaes.cornell.edu/pubs/press/1998/cider_uv_past.html. (2004/07/08)

Miller, R.V., W. Jeffrey, D. Mitchell and M. Elasri. 1999. Bacterial responses to ultraviolet light. *ASM News* 65(8): 535-541.

Mitscherlich, E. and E.H. Marth. 1984. *Microbial Survival in the Environment*. Berlin, Germany: Springer Verlag.

Nemeth, J. and G. Bucsky. 1997. Secondary flow generated in curved flow. *Hungarian Journal of Industrial Chemistry* 25: 91.

Qualls, R.G., M.P. Flynn and J.D. Johnson. 1983. The role of suspended particles in ultraviolet disinfection. *Journal of the Water Pollution Control Federation* 55(10): 1280-1285.

Rane, M.V. and M.S. Tandale. 2005. Water-to-water heat transfer in tube-tube heat exchanger: Experimental and analytical study. *Applied Thermal Engineering* 25 (17-18): 2715-2729.

Singh, R.K. and A.E. Ghaly. 1988. Cheese whey processing alternatives. ASAE Paper No. 88-6540. St. Joseph, MI: ASABE.

Singh, J.P. and A.E. Ghaly. 2006. Reduced fouling and enhanced microbial inactivation during online sterilization of cheese whey using UV coil reactors. *Bioprocess and Biosystems Engineering* 29(2): 269-281.

Tran, M.T.T. and M. Farid. 2004. Ultraviolet treatment of orange juice. *Innovative Food Science and Emerging Technologies* 5(4): 495-502.

USEPA. 1999. Wastewater technology fact sheet. Ultraviolet disinfection. EPA 832-F-99-064. Office of Water. Environmental Protection Agency, Washington, DC. http://www.epa.gov/owm/mtb/uv.pdf. (2004/06/04)

USEPA. 2002. The environmental technology verification program. Inactivation of MS2 virus in drinking water. NSF02/03/EPADWCTR. National Science Foundation, Washington, DC. http://www.epa.gov/etv/pdfs/vrvs/02_vr_trojan.pdf. (2005/11/10)

Van Osdell, D. and K. Foarde. 2002. Defining the effectiveness of UV lamps installed in circulating air ductwork. ARTI-21CR/610-40030-01. Final Report, prepared for the Air-Conditioning and Refrigeration Technology Institute, Arlington,VA.

Webster, D.R. and J.A.C. Humphrey. 1997. Traveling wave instability in helical coil flow. *Physics of Fluids* 9(2): 407-418.

LIST OF SYMBOLS

β volume coefficient of expansion (K^{-1})
Γ radius of curvature of spherical line cut out by helical element from tubular housing (m)
δ thickness of coil (m)
Δt time interval (h)
ρ_b density of material of reactor bottom (kg/m^3)
ρ_t density of material of reactor top (kg/m^3)
ρ_w density of the material of reactor walls (kg/m^3)
υ kinematic viscosity (m^2/s)
a tube diameter (m)
A_b surface area of the reactor bottom (m^2)
A_c annular section area (m^2)
A_{dw} cross-sectional area of cylinder (m^2)
A_{iw} surface area of inside wall of reactor (m^2)
A_{ow} surface area of outside wall of reactor (m^2)
A_t surface area of the reactor top (m^2)
A_w surface area of reactor outer walls (m^2)
b a parameter (m)
C_{bt} specific heat of bottom material of reactor ($kJ\ kg^{-1}\ K^{-1}$)
C_{pe} specific heat of effluent ($kJ\ kg^{-1}\ K^{-1}$)
C_{pt} specific heat of top material of reactor ($kJ\ kg^{-1}\ K^{-1}$)
C_w specific heat of wall material of reactor ($kJ\ kg^{-1}\ K^{-1}$)
d_b thickness of reactor bottom (m)
De Dean number
d_h hydraulic diameter (m)
d_i inner diameter (m)
d_o outer diameter (m)
d_t thickness of reactor top (m)
g gravitational acceleration (m/s^2)
Gr_f Grashof number
$Gr_f Pr_f$ Rayleigh number
h pitch of screw line (m)
h_{ib} convective heat transfer coefficient between inner surface of reactor bottom and cheese whey effluent ($kJ\ m^{-2}\ h^{-1}\ K^{-1}$)
h_{it} convective heat transfer coefficient between inner surface of reactor top and air in reactor ($kJ\ m^{-2}\ h^{-1}\ K^{-1}$)
h_{iw} convective heat transfer coefficient between cheese whey and reactor inside wall ($kJ\ m^{-2}\ h^{-1}\ K^{-1}$)
h_{ob} convective heat transfer coefficient between outer surface of reactor bottom and ambient air ($kJ\ m^{-2}\ h^{-1}\ K^{-1}$)
h_{ot} convective heat transfer coefficient between outer surface of reactor top and ambient air ($kJ\ m^{-2}\ h^{-1}\ K^{-1}$)
h_{ow} convective heat transfer coefficient between reactor outside wall and ambient air ($kJ\ m^{-2}\ h^{-1}\ K^{-1}$)
k_b thermal conductivity of bottom material ($kJ\ m^{-1}\ h^{-1}\ K^{-1}$)
k_t thermal conductivity of top material ($kJ\ m^{-1}\ h^{-1}\ K^{-1}$)
k_w thermal conductivity of cylindrical wall ($kJ\ m^{-1}\ h^{-1}\ K^{-1}$)
L_b characteristic length of reactor bottom diameter of bottom (m)
L_t characteristic length diameter of the top (m)
L_w characteristic length height of reactor (m)
M flow rate of effluent (kg/h)
m_b mass of bottom of reactor (kg)
m_t mass of top of reactor (kg)
m_w mass of walls of reactor (kg)
N final number of microorganisms
N_o initial number of microorganisms
q volumetric flow rate (m^3/s)
q_b rate of heat lost through reactor bottom (kJ/h)
q_e rate of heat lost with cheese whey effluent (kJ/h)
q_{gb} rate of heat gained by reactor bottom (kJ/h)
q_{gt} rate of heat gained by reactor top (kJ/h)
q_{gw} rate of heat gained by reactor walls (kJ/h)
q_r rate of heat gained by reactor components (kJ/h)
q_t rate of heat lost through reactor top (kJ/h)
q_u rate of heat generated by UV lamp (kJ/h)
q_w rate of heat lost through reactor walls (kJ/h)
r tube radius (m)
Re Reynolds number
r_i inner radius of reactor (m)
r_o outer radius of reactor (m)
r^x radius of circle having same surface as area of half cross-section beside static element (m)
T_1 initial temperature (K)
T_2 final temperature (K)
T_a ambient air temperature (K)
T_f film temperature
T_i inlet temperature of cheese whey (K)
T_{ia} temperature of air entrapped in head space of reactor (K)
T_{ie} inlet temperature of effluent (K)
T_{it} temperature of inside surface of reactor top (K)
T_m mean temperature of cheese whey (K)
T_{ob} temperature of the surface of the bottom (K)
T_{oe} outlet temperature of effluent (K)
T_{ot} temperature on outside surface of reactor top (K)
T_{ow} temperature of outer surface of reactor wall (K)
U mean velocity (m/s)
U_b overall heat transfer coefficient of reactor bottom ($kJ\ m^{-2}\ h^{-1}\ K^{-1}$)
U_t overall heat transfer coefficient of reactor top ($kJ\ m^{-2}\ h^{-1}\ K^{-1}$)
U_w overall heat transfer coefficient of reactor walls ($kJ\ m^{-2}\ h^{-1}\ K^{-1}$)